

Switchable iridium hydride catalysts for controlling selectivity of alcohol oxidation

Marta Olivares^a and Martin Albrecht^{*,a}

^a Departement für Chemie und Biochemie, Universität Bern, Freiestrasse 3, CH-3012 Bern, Switzerland

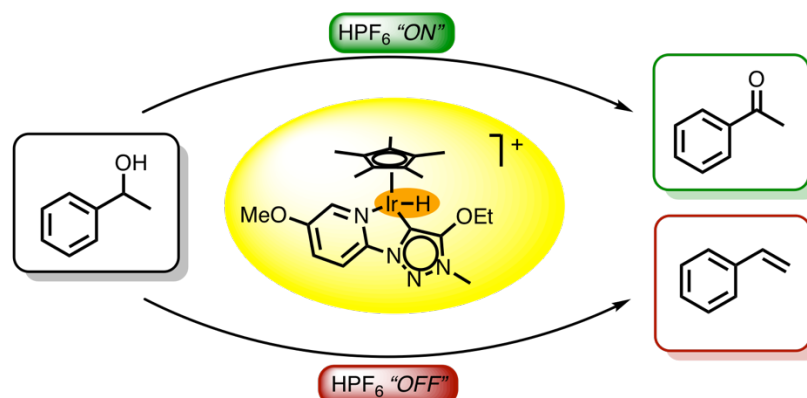
* to whom correspondence should be addressed:

martin.albrecht@dcb.unibe.ch;

dedicated to Prof. F. E. Hahn on the occasion of his 65th birthday and in recognition of his inspiring work in N-heterocyclic carbene chemistry

Abstract

Novel pyridyl-triazolylidene iridium(III) hydride complexes have been synthesized through modification of the analogous iridium chloride complexes. The dehydration of alcohols was used to probe the catalytic potential of the iridium chloride compounds and the influence of the electronic modification on the pyridyl-triazolylidene ligand scaffolds. The incorporation of electron donor substituents on the triazolylidene heterocycle considerably enhanced the catalytic activity of the coordinated iridium center towards the catalytic dehydration of alcohols. Moreover, the iridium hydride compounds are switchable catalysts that perform either alcohol dehydration or dehydrogenation. Their selectivity was predictably triggered by the presence or absence of HPF_6 in the catalytic reaction.



Introduction

The design and synthesis of efficient catalysts that generate valuable products from cheap, abundant and inert materials is a challenging task in chemistry. Particularly attractive are switchable catalysts[1–6] that enable different conversions of a single substrate triggered by an external stimulus such as pH change,[7–9] solvents,[10,11] heat and/or light,[12–16] or other modifications of reaction conditions.[1,17,18] For example, switching of solvent ionicity by addition and removal of CO₂ to an amine solvent[19] provided control over ring-opening polymerization activity.[20]

Such ligand switchability has also been implemented with catalysts comprising N-heterocyclic carbene (NHC) ligands. Early work included the introduction of proton-responsive aminophenyl substituents on Grubbs- and Hoveyda-Grubbs-type catalysts which allowed the catalytic ring-opening metathesis polymerization activity to be controlled by pH modifications.[21–23] More recently, this concept has been elegantly expanded to afford redox- and light-switchable NHC ruthenium catalysts that respond to stimuli changes, for example to toggle between ring-opening and ring closing olefin metathesis reactions.[24–27]

We recently showed switchable and multitasking catalytic properties of an iridium(Cp*) complex containing a triazolylidene ligand, a subclass of N-heterocyclic carbenes (NHCs).[28,29] Depending on the reaction conditions, this complex converts ketones either reductively via hydrosilylation or promotes deoxidative olefin formation as well as the production of ethers.[30,31] Here we introduce related triazolylidene iridium hydride complexes which switch catalytic selectivity in the conversion of alcohols between dehydration (loss of H₂O) and dehydrogenation (loss of H₂), which is triggered by the presence or absence of an acid. The easy accessibility of these 1,2,3-triazolylidene ligands by mild and functional-group tolerant copper-catalyzed click reaction[32] has been exploited to modulate the electronic properties as a methodology to tailor the catalytic performance. Specifically, complexes **1–4** were considered[33] as they are comprised of a variety of electronically active groups on the triazolylidene unit including an electron-donating ethoxy substituent (complex **1**), a neutral triazolylidene (complex **2**), and electron-withdrawing carboxylate without and with protic characteristics (complexes **3** and **4**, respectively).

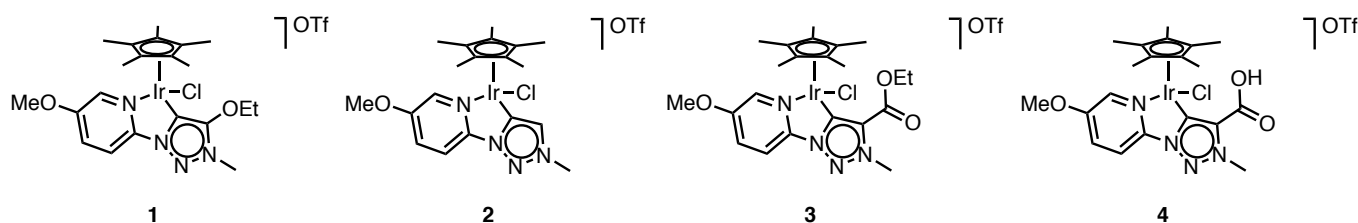


Figure 1. Set of iridium complexes containing electronically variable substituents on the triazolylidene unit used for catalytic application.

Result and discussion

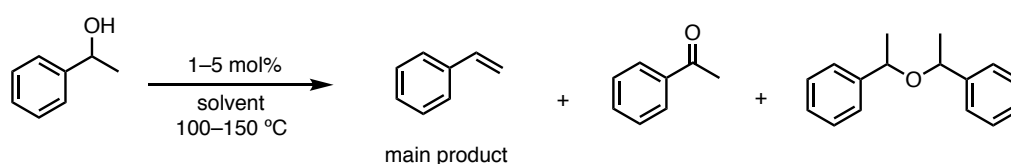
1. Dehydration of 1-phenylethanol and other alcohols

The catalytic activity of complexes **1–4** towards alcohol conversion was evaluated using 1-phenylethanol as model substrate and 1,2-dichlorobenzene as solvent.[34–37] An initial run using complex **1** at 5 mol% loading produced styrene, as the major product in 77% yield after 1 h. In addition, minor quantities of ether as the alternative product of dehydration as well as acetophenone were also observed in 5% and 10% yield, respectively (entry 1, Table 1), indicating that dehydration is the major reaction pathway, though dehydrogenation is feasible. After 2 h, all the substrate was consumed and styrene was the main product (95% yield) together with traces of ether and ketone (2% and 3%, respectively; entry 2). After 4 h, the selectivity increased further with essentially quantitative formation of styrene and less than 2% ether (entry 3). It is interesting to note that the initially formed ketone — as much as 10% after 1 h — was completely consumed, and also the amount of ether gradually decreased from 5% to less than 2%, suggesting that both ether and ketone are transformed under the reaction conditions. Similar results were obtained when lowering the catalyst loading to 1 mol%. Conversion reached 55% after 30 min and full conversion after 2 h (entries 4, 5). Styrene was the major product and the initially notable amount of ether (6%) decreased to 2%, together with some ketone (6%).

The role of the iridium complex was evaluated by comparing the catalytic activity of complex **1** to complexes **2–4** with steric and electronic modifications of the triazolylidene ligand. At 1 mol% catalyst loading, complex **2** without a substituent on the triazolylidene scaffold showed slightly lower activity (48% vs 55% with complex **1** after 30 min), while complex **3** was less active and reached only 31% conversion in the same time span (entries 6,7). Interestingly, complex containing a carboxylic acid group did not show any catalytic activity (entry 8), indicating that mild acids are inhibiting catalytic turnover. The increase of catalytic activity from complex **3** to **2** to **1** correlates with the substituent-induced enhanced donor properties of the triazolylidene ligand (R = COOEt, H, OEt along this series). The change in activity has, however, no influence

on the selectivity and all complexes form predominantly styrene due to alcohol dehydration, together with minor quantities of ether (<6%). However, the selectivity is directly affected by changes in the reaction conditions. Thus, decreasing the temperature from 150 °C to 100 °C reduced the conversion from 99% to 65% conversion after 4 h and gave considerably higher quantities ketone (20%) and ether (15%) compared to runs at higher temperature (entry 9; *cf* entry 3). Further lowering of the reaction to room temperature was ineffective and led to a complete cessation of catalytic activity.

Table 1. Catalytic activity of complexes **1–4** in dehydration catalysis of 1-phenylethanol.^a



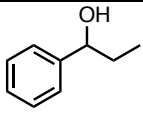
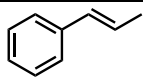
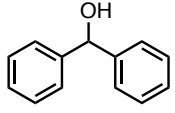
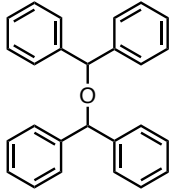
entry	complex	cat. loading	time (h)	conv. (%)	yield (%)		
					styrene	ketone	ether
1	1	5 mol%	1	91	77	10	5
2	1	5 mol%	2	>99	95	3	2
3	1	5 mol%	4	>99	98	–	2
4	1	1 mol%	0.5	55	49	–	6
5	1	1 mol%	2	>99	92	6	2
6	2	1 mol%	0.5	48	41	1	6
7	3	1 mol%	0.5	31	27	–	4
8	4	1 mol%	0.5	–	–	–	–
9 ^b	1	5 mol%	4	65	30	20	15

^a General reaction conditions: 1-phenylethanol (0.2 mmol), 1,2-dichlorobenzene (2 mL), 150 °C, under inert conditions. Conversions were determined by ¹H NMR integration (anisole as internal standard). ^b Reaction run at 100 °C.

The activity of complex **1** is strongly substrate dependent. For example, 1-phenyl-1-propanol also underwent dehydration and formed β -methyl styrene in high selectivity, though conversion only reached 58% after 2 h (Table 2, entry 1; *cf* full conversion with 1-phenyl-1-ethanol, Table 1). Reaction of 1,1-diphenylmethanol led to quantitative formation of the ether within 2 h as product of dehydration, since olefin formation is not possible with this substrate (entry 2). Complex **1** was inactive towards 4-phenyl-2-butanol as an aliphatic alcohol as well as towards α -methylbenzylamine. The specific selectivity of these iridium complexes towards benzylic

alcohols may become attractive with more complex substrates containing a variety of functional groups.

Table 2. Reactivity of complex **1** towards different substrates.^a

entry	substrate	product	yield (%)
1			58
2			95

^aGeneral reaction conditions: Substrate (0.2 mmol), **1** (0.002 mmol, 1 mol%), 1,2-dichlorobenzene (2 mL), 150 °C, 2 h reaction under inert conditions. Conversions were determined by ¹H NMR integration (anisole as internal standard).

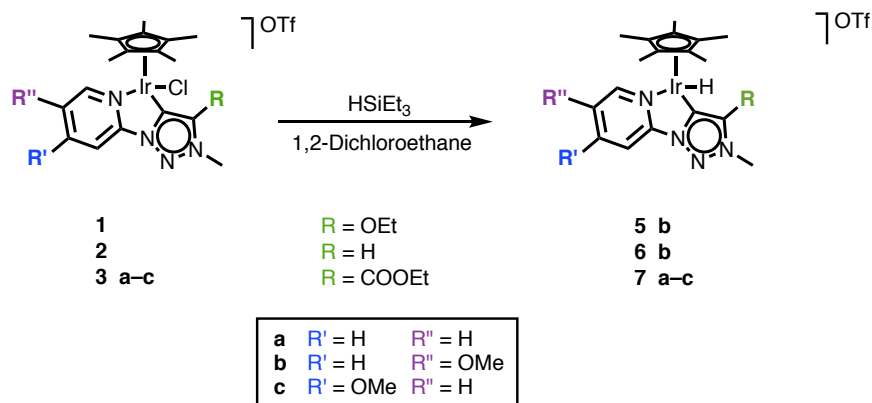
2. Synthesis of pyridyl-triazolylidene iridium hydride complexes

The formation of ketones, albeit in low yield, suggests the transient formation of a hydride species. In an effort to gain mechanistic insights as well as to potentially enhance the catalytic activity of the complex, we sought to prepare iridium hydrides as catalyst precursors. Specifically, iridium hydride complexes potentially provide access to dehydrogenation pathways through reaction of the metal hydride with the alcohol OH group to release H₂. Therefore, the iridium hydride complexes **5–7** were prepared from the corresponding iridium chloride complexes by employing a slightly modified literature procedure (Scheme 1).[38] Accordingly, complexes **1–3** were heated in 1,2-dichloroethane in the presence of an excess of triethylsilane (10 eq) for 2 h at 100 °C and for another 2 h at room temperature (Scheme 1). Precipitation and repetitive washing with Et₂O to remove excess silane as well as the ClSiEt₃ by-product afforded complexes **5–7** in moderate 35–50% yield. The reaction was monitored by ¹H NMR spectroscopy as formation of the iridium hydride was indicated by a diagnostic high-field resonance around –14 ppm. Of note, a large excess of HSiEt₃ was necessary for the reaction to run to completion. When using only 2 equivalents of silane, partial hydride formation was observed within 90 min, however, these hydride species subsequently converted back to the iridium chloride starting complex.

Formation of the iridium hydride complexes was also observed by NMR spectroscopy when complexes **1–3** were treated with KBH₄ (5 eq) in a mixture of CD₃CN:CD₃OD (1:1). However, these reaction conditions induced isotope exchange of Ir–H to Ir–D, as indicated by the gradual disappearance of the resonance at δ_H = –14.2 ppm for complex **6**. Addition of 10 μL of H₂O

reverted the isotope exchange and the hydride resonance was recovered. The hydride complexes generated from KBH_4 were only stable in the crude reaction mixture. All attempts to isolate and purify the hydride complex resulted in decomposition.

Scheme 1. Synthesis of iridium hydride complexes **5–7**.



All complexes **5–7** were unstable in deuterated dichloromethane and 1,2-dichloroethane. In these solvents chloride abstraction was observed with gradual formation of the chloride complexes **1–3** within 16 h, identifying the hydride formation with HSiEt_3 in dichloroethane as an equilibrium reaction. Such an equilibrium is in line with the observation that the reaction is only partially complete when using 2 equiv. HSiEt_3 and rationalizes the large excess of HSiEt_3 required to reach full conversion to the hydride when the reaction is carried out in chlorinated solvent.

Full NMR spectroscopic characterization of complexes **5–7** was therefore carried out in CD_3CN solution. All complexes show the characteristic hydride resonance around -14 ppm. The exact resonance frequency of this signal is, however, not correlated to the electronics of the pyridyl-triazolylidene ligand. For example complexes **5**, **6**, and **7b** all feature the same 5-methoxy-pyridyl unit and differ only in the substituent R of the triazole heterocycle. The hydride resonance of these complexes shifts upfield from $\delta_{\text{H}} = -13.80$ in **7b** with electron-withdrawing COOEt substituent to -14.18 for complex **6** without an electronically active substituent ($\text{R} = \text{H}$; Table 3). However, introducing an electron-donating substituent (complex **5**, $\text{R} = \text{OEt}$) induces a downfield shift ($\delta_{\text{H}} = -13.86$). Likewise, no trend was observed when comparing the chemical shifts of the hydrides in complexes **7a–c**, which contain the same COOEt -substituted triazolylidene fragment and only differ in the substitution pattern of the pyridyl unit. Complex **7a** without a methoxy group shows the hydride at the lowest field in this series. Even though the Hammett parameter of the OMe group is positive when *meta*-substituted and negative when *para*-substituted, both complexes **7b** and **7c** displayed the hydride resonance at higher field ($\delta_{\text{H}} = -13.80$ and -13.93 , respectively).

Table 3. Selected ^1H NMR chemical shifts for complexes **5–7**^a

Complex	^1H NMR (ppm)	
	Ir–H	NCH ₃
5	–13.86	4.07
6	–14.18	4.27
7a	–13.70	4.44
7b	–13.80	4.42
7c	–13.93	4.43

^a in CD₃CN at 300 MHz.

While the electronic effects from ligand modification is not linear for the hydride NMR frequency, it is evident on the heterocycle itself as demonstrated with the gradual downfield shift of the N–CH₃ resonance when comparing complexes **5** (R = OEt, $\delta_{\text{H}} = 4.07$), **6** (R = H, $\delta_{\text{H}} = 4.27$), and **7b** (R = COOEt, $\delta_{\text{H}} = 4.42$).

Complexes **6** and **7b** were further characterized by single crystal X-ray diffraction analysis. Suitable crystals were grown by diffusion of Et₂O into a saturated CH₃CN solution of the corresponding complex. Both iridium hydride complexes display the typical three-legged piano-stool geometry of Ir(Cp*) complexes (Figure 2).[33,39] The hydrides were refined with a constrained Ir–H distance (1.61 ± 0.04 Å) to avoid divergence. The C_{trz}–Ir–N_{py} bite angle of the chelating ligand is 77.21(2) and 78.21(1) in complexes **6** and **7b**, respectively (Table 4), and hence slightly larger than in the analogous iridium chloride complexes ($76.9(5)^\circ$),[33] and other transition metal complexes bearing pyridyl-triazolylidene ligands.[39] This widening of the bite angle is due to slightly shorter Ir–N_{py} and Ir–C_{trz} bonds in the iridium hydride complexes (2.09(1) and 2.006(6) Å, respectively) compared to the chloride analogues (2.12(4) and 2.03(4) Å respectively).[33] This contraction is attributed to the nature of the anionic ligand (Cl[–] vs H[–]).

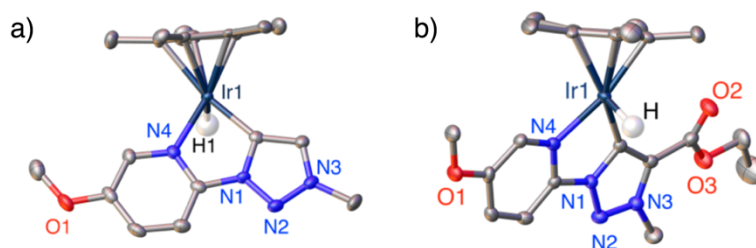
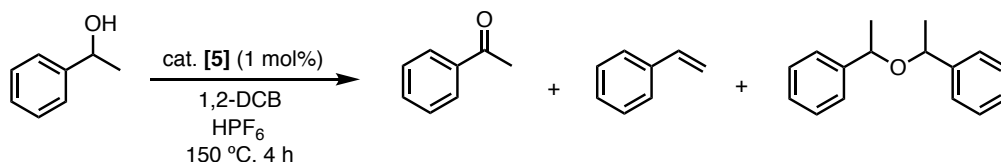
**Figure 2.** Schematic drawing and ORTEP plots for complexes **6** (a) and **7b** (b; both 50% probability ellipsoids, non-coordinating OTf[–] anions and all hydrogens except the metal-bound hydride omitted for clarity). The hydride has not been refined from the difference Fourier map and was inserted at calculated position.

Table 4. Selected bond lengths (Å) and angles (°) for complexes **6** and **7b**.

Complex	6	7b
Ir–N _{py}	2.087(4)	2.101(3)
Ir–C _{trz}	2.001(4)	2.012(4)
Ir–Cp* _{centr}	1.848(3)	1.859(2)
C _{trz} –C _{trz}	1.379(7)	1.408(5)
C _{trz} –Ir–N _{py}	77.205(16)	78.212(13)

3. Catalytic activity of hydride complexes towards 1-phenylethanol

The catalytic activity of complex **5** in alcohol dehydrogenation reaction was evaluated by using 1-phenylethanol as a model substrate. Complex **5** was selected as the chloride complex with the analogously substituted pyridyl-triazolyldiene ligand was the most active species in the series for dehydration reactions (see above). At 1 mol% catalyst loading the iridium hydride complex **5** displayed catalytic activity and selectivity that are similar to the iridium chloride complex **1**, reaching 89% conversion within 2 h and yielding 83% styrene with traces of ether (entry 1, Table 5). The fact that both complexes **1** and **5** show essentially identical catalytic profiles points to the formation of the same catalytic species under standard reaction conditions.

Table 5. Catalytic dehydrogenation of 1-phenylethanol.^a

entry	HPF ₆ (eq)	conv. (%)	yield (%)			selectivity (%) ^b
			ketone	styrene	ether	
1 ^c	–	89	–	83	6	0
2	3	>99	24	76	–	24
3	6.2	93	53	37	3	57
4	8	96	35	57	4	38
5	10	96	34	59	3	35
6 ^d	6.2	96	40	52	4	42
7 ^d	10	>99	18	82	–	18
8 ^e	6.2	>99	<2	98	–	<2
9	2+2	61	34	21	6	56
10 ^f	6.2	>99	–	60	–	0

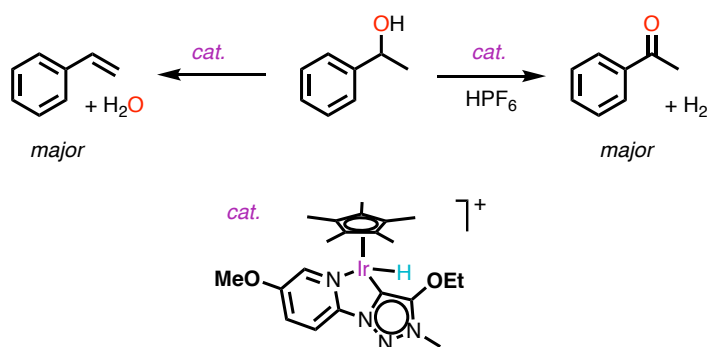
^a General reaction conditions: 1-phenylethanol (0.2 mmol), complex **5** (0.002 mmol, 1 mol%) and 1,2-dichlorobenzene (2 mL), 150 °C, 4 h, under inert conditions. Conversions determined by ¹H NMR integration (anisole as the internal standard). ^b Selectivity towards dehydrogenation (ketone formation).

^c Conversion and yield after 2 h reaction. ^d 1-phenylethanol was added after heating the reaction mixture for 5 min. ^e Complex **1** was used as catalyst precursor. ^f No complex added.

In order to investigate the role of the hydride and a potential *in situ* formed solvento species, HPF₆ was used as a hydride abstractor with complex **5**. Dihydrogen formation with HPF₆ produces a non-coordinating anion that was assumed to have no interference with the metal center in catalysis. Addition of 3 mol% HPF₆ (3:1 ratio of acid to iridium hydride) increased the conversion to completeness and altered the selectivity, as acetophenone was produced in 24% in addition to styrene (entry 2). In the absence of acid, no ketone was produced. Monitoring of the reaction of complex **5** with HPF₆ by ¹H NMR spectroscopy (CD₃CN) indeed revealed a rapid loss of the characteristic hydride resonance at -13.86 ppm, which supports the release of the hydride and the formation of the solvento complex as first step for the alcohol dehydrogenation reaction. Concomitantly, most ligand signals shift to slightly lower field, which is indicative of a change in the metal coordination sphere.

Variation of the concentration of HPF₆ allowed to further modulate the selectivity (entries 3–7). Thus, an increase in HPF₆ from 3 to 6.2 mol% enhanced the formation of the ketone product to 53% together with 37% of styrene as well as traces of ether (57% selectivity towards acetophenone, entry 3), indicating an acid-mediated switch of selectivity of iridium complex **5** from dehydration to dehydrogenation (Scheme 2). A further increase of HPF₆ to 8 and 10 mol% led to a drop in selectivity to about 35%, indicating that there is an optimum acid concentration for maximizing selectivity, and that higher acid concentrations promote the formation of styrene (entries 4, 5). Pre-activation of the catalyst, by heating the complex with HPF₆ in 1,2-DCB at 150 °C for 5 min before adding the alcohol substrate decreased the formation of ketone, presumably because the formed cationic species is not sufficiently stabilized (entries 6, 7). Instead, HPF₆ may thermally decompose to HF and PF₅,^[40] which is supposed to produce the analogous Ir-F complex with selectivity towards styrene production analogous to complex **1**. A control experiment using the iridium chloride complex **1** in presence of HPF₆ afforded almost exclusively styrene with only traces of ketone (<2%, entry 8), indicating that halide coordination is prohibiting alcohol dehydrogenation. In addition, the distinct selectivity of complexes **1** and **5** under acidic conditions reveals the relevance of the hydride and hydride activation for shifting the selectivity towards dehydrogenation.

Scheme 2. Acid-triggered switch of product selectivity in the transformation of alcohols with iridium hydride complex **5**, inducing predominantly dehydration vs dehydrogenation.



Addition of the acid in portions, *viz.* 2 eq at the beginning and 2 further eq after one hour, slows down substrate conversion considerably and produced only 61% conversion after 4 h, indicating substantial catalyst deactivation even though selectivity towards dehydrogenation remained at 56% (entry 9), *i.e.* the same level as when adding 6 mol% acid at the reaction onset (*cf* entry 3). A blank reaction using just HPF_6 yet no complex **5** revealed the full consumption of the substrate after 2 h and formation predominantly of styrene (entry 10). Dehydration of alcohols by strong acids via protonation followed by elimination of H_2O is well known[41,42] and rationalizes the dual role of HPF_6 in this process: on one hand side, it is required to abstract the iridium-bound hydride to form the dehydrogenation catalyst, while on the other hand side it induces a non-metal catalyzed dehydration which compromises selectivity. Hence, there is an optimum iridium:acid ratio for promoting dehydrogenation with these iridium hydride complexes.

Conclusions

Functionalized pyridyl-triazolylidene iridium chloride complexes have been demonstrated to catalyze alcohol dehydration. Tailoring of catalytic activity was accomplished by modification of the donor properties of the triazolylidene ligand and revealed a direct correlation between the ligand electronic properties and the catalytic performance, with stronger donors increasing activity. The corresponding iridium hydride complexes catalyze both the dehydration as well as the dehydrogenation of alcohols. Their activity is switched by the presence/absence of HPF_6 . Such multipurpose catalysis is attractive for the valorization of abundant feedstock chemicals.

Experimental section

General. The syntheses of the hydride compounds were carried out in the glove box, and all the solvents were dried under active molecular sieves and degassed using freeze-pump-thaw techniques. Complexes **1–4** were prepared according to literature procedure.[33] Unless specified, NMR spectra were recorded at 25 °C on Bruker spectrometers operating at 300 MHz (^1H NMR) and 75 MHz (^{13}C NMR), respectively. Chemical shifts (δ in ppm, coupling constants

J in Hz) were referenced to residual solvent signals (^1H , ^{13}C). Assignments are based on homo- and heteronuclear shift correlation spectroscopy. All complexes show a quartet around 120 ppm in the ^{13}C NMR spectrum due to the OTf^- counterion. Purity of the complexes has been established by NMR spectroscopy.

General procedure for the synthesis of the complexes 5–7: In a Schlenk flask in the glove box, compound 1–3 (1 eq) and HSiEt_3 (10 eq) were suspended in dry 1,2-dichloroethane (1.5 mL) and stirred for 2 h at 100 °C and for another 2 h at room temperature. The reaction mixture was layered with dry Et_2O , which induced precipitation of complexes 5–7 as yellow solids.

Complex 5: Reaction of complex 1 (60 mg, 0.08 mmol) and HSiEt_3 (100 μL , 0.80 mmol) were suspended in dichloroethane (1.5 mL) and stirred according to the general procedure to obtain complex 5 as a yellow solid. Yield 28 mg, 49%. ^1H NMR (300 MHz, CD_3CN): δ = 8.35 (s, 1H, $\text{C}_{\text{py}}\text{H}$), 7.99 (d, $^3J_{\text{HH}} = 9.0$ Hz, 1H, $\text{C}_{\text{py}}\text{H}$), 7.69 (d, $^3J_{\text{HH}} = 9.0$ Hz, 1H, $\text{C}_{\text{py}}\text{H}$), 4.45–4.13 (m, 2H, OCH_2Me), 4.07 (s, 3H, NCH_3), 3.99 (s, 3H, OCH_3), 1.99 (s, 15H, Cp-CH_3), 1.42 (t, $^3J_{\text{HH}} = 7.3$ Hz, 3H, OCH_2CH_3), -13.86 (s, 1H, Ir-H). $^{13}\text{C}\{^1\text{H}\}$ NMR (75 MHz, CD_3CN): δ = 157.7 ($\text{C}_{\text{py-O}}\text{Me}$), 156.9 ($\text{C}_{\text{trz-Ir}}$), 145.7 ($\text{C}_{\text{py-N}}\text{trz}$), 139.9 ($\text{C}_{\text{py}}\text{H}$), 138.9 ($\text{C}_{\text{trz-OEt}}$), 126.2 ($\text{C}_{\text{py}}\text{H}$), 114.5 ($\text{C}_{\text{py}}\text{H}$), 92.8 (Cp^*), 73.6 (OCH_2Me), 57.6 (OCH_3), 35.7 (NCH_3), 15.2 (OCH_2CH_3), 10.4 (Cp-CH_3). HR-MS (CH_3CN): m/z calculated for $\text{C}_{21}\text{H}_{30}\text{N}_4\text{O}_2\text{Ir} [\text{M-OTf}]^+ = 563.1993$; found, 563.1999.

Complex 6: Complex 2 (60 mg, 0.085 mmol) and HSiEt_3 (100 μL , 0.85 mmol) were stirred according to the general procedure to obtain complex 6. Yield 25 mg, 44%. ^1H NMR (300 MHz, CD_3CN): δ = 8.35 (d, $^4J_{\text{HH}} = 2.6$ Hz, 1H, $\text{C}_{\text{py}}\text{H}$), 8.01 (d, $^3J_{\text{HH}} = 9.2$ Hz, 1H, $\text{C}_{\text{py}}\text{H}$), 7.89 (s, 1H, $\text{C}_{\text{trz}}\text{H}$), 7.69 (dd, $^3J_{\text{HH}} = 9.2$ Hz, $^4J_{\text{HH}} = 2.6$ Hz, 1H, $\text{C}_{\text{py}}\text{H}$), 4.27 (s, 3H, NCH_3), 3.99 (s, 3H, OCH_3), 1.99 (s, 15H, Cp-CH_3), -14.18 (s, 1H, Ir-H). $^{13}\text{C}\{^1\text{H}\}$ NMR (75 MHz, CD_3CN): δ = 157.5 ($\text{C}_{\text{py-O}}\text{Me}$), 154.3 ($\text{C}_{\text{trz-Ir}}$), 145.3 ($\text{C}_{\text{py-N}}\text{trz}$), 140.0 ($\text{C}_{\text{py}}\text{H}$), 132.2 ($\text{C}_{\text{trz}}\text{H}$), 126.0 ($\text{C}_{\text{py}}\text{H}$), 114.9 ($\text{C}_{\text{py}}\text{H}$), 92.8 (Cp^*), 57.6 (OCH_3), 40.1 (NCH_3), 10.2 (Cp-CH_3). Anal. Calcd for $\text{C}_{20}\text{H}_{26}\text{F}_3\text{IrN}_4\text{O}_4\text{S}$ (667.72): C, 35.98; H, 3.92; N, 8.39. Found: C, 35.66; H, 3.86; N, 8.16. HR-MS (CH_3CN): m/z calculated for $\text{C}_{19}\text{H}_{26}\text{N}_4\text{OIr} [\text{M-OTf}]^+ = 519.1736$; found, 519.1713.

Complex 7a: Reaction of complex 3a (40 mg, 0.05 mmol) and HSiEt_3 (86 μL , 0.54 mmol) were stirred according to the general procedure to afford 7a as a yellow solid. Yield 17 mg, 48%. ^1H NMR (300 MHz, CD_3CN): δ = 8.82 (d, $^3J_{\text{HH}} = 5.8$ Hz, 1H, $\text{C}_{\text{py}}\text{H}$), 8.13–7.95 (m, 2H, $\text{C}_{\text{py}}\text{H}$), 7.49 (ddd, $^3J_{\text{HH}} = 7.4$ Hz, $^3J_{\text{HH}} = 5.8$ Hz, $^4J_{\text{HH}} = 1.8$ Hz, 1H, $\text{C}_{\text{py}}\text{H}$), 4.68–4.44 (m, 2H, OCH_2Me) 4.44 (s, 3H, NCH_3), 1.94 (s, 15H, Cp-CH_3), 1.44 (t, $^3J_{\text{HH}} = 7.1$ Hz, 3H, OCH_2CH_3), -13.93 (s, 1H,

Ir–H). $^{13}\text{C}\{^1\text{H}\}$ NMR (75 MHz, CD_3CN): $\delta = 159.8$ ($\text{C}_{\text{trz}}\text{–Ir}$), 159.3 (C=O), 153.6 ($\text{C}_{\text{py}}\text{H}$), 150.9 ($\text{C}_{\text{py}}\text{–N}_{\text{trz}}$), 140.8 ($\text{C}_{\text{py}}\text{H}$), 136.8 ($\text{C}_{\text{trz}}\text{–COOEt}$), 126.6 ($\text{C}_{\text{py}}\text{H}$), 114.8 ($\text{C}_{\text{py}}\text{H}$), 93.7 (Cp^*), 63.9 (OCH_2Me), 42.6 (NCH_3), 14.4 (OCH_2CH_3), 10.3 ($\text{Cp}\text{–CH}_3$). Anal. Calcd for $\text{C}_{22}\text{H}_{28}\text{F}_3\text{IrN}_4\text{O}_5\text{S}$ (709.76): C, 37.23; H, 3.98; N, 7.89. Found: C, 36.52; H, 3.69; N, 7.62. HR-MS (CH_3CN): m/z calculated for $\text{C}_{21}\text{H}_{28}\text{N}_4\text{O}_2\text{Ir} [\text{M}\text{–OTf}]^+ = 561.1836$; found, 561.1827.

Complex 7b: Complex **3b** (60 mg, 0.077 mmol) and HSiEt_3 (125 μL , 0.77 mmol) were stirred according to the general procedure to give **7b**. Yield 21 mg, 37%. ^1H NMR (300 MHz, CD_3CN): $\delta = 8.41$ (d, $^4J_{\text{HH}} = 2.6$ Hz, 1H, $\text{C}_{\text{py}}\text{H}$), 8.08 (d, $^3J_{\text{HH}} = 9.2$ Hz, 1H, $\text{C}_{\text{py}}\text{H}$), 7.72 (dd, $^3J_{\text{HH}} = 9.2$ Hz, $^4J_{\text{HH}} = 2.6$ Hz, 1H, $\text{C}_{\text{py}}\text{H}$), 4.64–4.44 (m, 2H, OCH_2Me), 4.42 (s, 3H, NCH_3), 4.01 (s, 3H, OCH_3), 1.94 (s, 15H, $\text{Cp}\text{–CH}_3$), 1.44 (t, $^3J_{\text{HH}} = 7.1$ Hz, 3H, OCH_2CH_3), -13.70 (s, 1H, Ir–H). $^{13}\text{C}\{^1\text{H}\}$ NMR (75 MHz, CD_3CN): $\delta = 159.4$ (C=O), 158.0 ($\text{C}_{\text{trz}}\text{–Ir}$), 157.7 ($\text{C}_{\text{py}}\text{–OMe}$), 144.7 ($\text{C}_{\text{py}}\text{–N}_{\text{trz}}$), 139.6 ($\text{C}_{\text{py}}\text{H}$), 136.7 ($\text{C}_{\text{trz}}\text{–COOEt}$), 126.5 ($\text{C}_{\text{py}}\text{H}$), 115.1 ($\text{C}_{\text{py}}\text{H}$), 93.6 (Cp^*), 63.8 (OCH_2Me), 57.6 (OCH_3), 42.4 (NCH_3), 14.5 (OCH_2CH_3), 10.3 ($\text{Cp}\text{–CH}_3$). HR-MS (CH_3CN): m/z calculated for $\text{C}_{22}\text{H}_{30}\text{N}_4\text{O}_3\text{Ir} [\text{M}\text{–OTf}]^+ = 591.1947$; found, 591.1933.

Complex 7c: Reaction of complex **3c** (40 mg, 0.052 mmol) and HSiEt_3 (83 μL , 0.52 mmol) were suspended in 1,2-dichloroethane (1 mL) and stirred according to the general procedure to afford complex **7c** as a yellow solid. Yield 14 mg, 36%. ^1H NMR (300 MHz, CD_3CN): $\delta = 8.53$ (d, $^3J_{\text{HH}} = 6.7$ Hz, 1H, $\text{C}_{\text{py}}\text{H}$), 7.67 (d, $^4J_{\text{HH}} = 2.6$ Hz, 1H, $\text{C}_{\text{py}}\text{H}$), 7.08 (dd, $^3J_{\text{HH}} = 6.7$ Hz, $^4J_{\text{HH}} = 2.6$ Hz, 1H, $\text{C}_{\text{py}}\text{H}$), 4.63–4.45 (m, 2H, OCH_2Me), 4.43 (s, 3H, NCH_3), 4.03 (s, 3H, OCH_3), 1.93 (s, 15H, $\text{Cp}\text{–CH}_3$), 1.44 (t, $^3J_{\text{HH}} = 7.1$ Hz, 3H, OCH_2CH_3), -13.80 (s, 1H, Ir–H). $^{13}\text{C}\{^1\text{H}\}$ NMR (75 MHz, CD_3CN): $\delta = 169.3$ ($\text{C}_{\text{py}}\text{–OMe}$), 160.3 ($\text{C}_{\text{trz}}\text{–Ir}$), 159.2 (C=O), 153.5 ($\text{C}_{\text{py}}\text{H}$), 151.9 ($\text{C}_{\text{py}}\text{–N}_{\text{trz}}$), 136.8 ($\text{C}_{\text{trz}}\text{–COOEt}$), 113.9 ($\text{C}_{\text{py}}\text{H}$), 100.0 ($\text{C}_{\text{py}}\text{H}$), 93.1 (Cp^*), 63.7 (OCH_2Me), 57.9 (OCH_3), 42.5 (NCH_3), 14.3 (OCH_2CH_3), 10.2 ($\text{Cp}\text{–CH}_3$). Anal. Calcd for $\text{C}_{23}\text{H}_{30}\text{F}_3\text{IrN}_4\text{O}_6\text{S}$ (739.79): C, 37.34; H, 4.09; N, 7.57. Found: C, 37.15; H, 4.01; N, 7.36. HR-MS (CH_3CN): m/z calculated for $\text{C}_{22}\text{H}_{30}\text{N}_4\text{O}_3\text{Ir} [\text{M}\text{–OTf}]^+ = 591.1947$; found, 591.1921.

Typical procedure for the dehydration of 1-phenylethanol (1 mol% catalyst loading). Complex **1–4** (0.002 mmol), anisole (internal standard, 22 μL , 0.2 mmol), 1-phenylethanol (24 μL , 0.2 mmol) and 1,2-dichlorobenzene (2 mL) were placed in a closed vial under nitrogen and heated at 150 $^\circ\text{C}$. An aliquot (0.1 mL) was taken at fixed times, diluted with CDCl_3 (0.5 mL), and analyzed by ^1H NMR spectroscopy.

Typical procedure for the dehydration of 1-phenylethanol (5 mol% catalyst loading). Complex **1** (7.5 mg, 0.01 mmol), anisole (internal standard, 22 μL , 0.2 mmol), 1-phenylethanol

(24 μL , 0.2 mmol) and 1,2-dichlorobenzene (2 mL) were placed in a closed vial under nitrogen and heated at 150 $^{\circ}\text{C}$. An aliquot (0.1 mL) was taken at fixed times, diluted with CDCl_3 (0.5 mL), and analyzed by ^1H NMR spectroscopy.

Typical procedure for the dehydrogenation of 1-phenylethanol. Complex **5** (1.4 mg, 0.002 mmol), anisole (internal standard, 22 μL , 0.2 mmol), 1-phenylethanol (24 μL , 0.2 mmol), 1,2-dichlorobenzene (2 mL) and HPF_6 (3–10 eq) were placed in a closed vial under nitrogen and heated at 150 $^{\circ}\text{C}$. An aliquot (0.1 mL) was taken at fixed times, diluted with CDCl_3 (0.5 mL), and analyzed by ^1H NMR spectroscopy.

Crystallographic details. All measurements were made on an Oxford Diffraction SuperNova area-detector diffractometer[43] using mirror optics monochromated Mo $K\alpha$ radiation ($\lambda = 0.71073 \text{ \AA}$) and Al filtered.[44] Data reduction was performed using the CrysAlisPro program. The intensities were corrected for Lorentz and polarization effects, and numerical absorption correction based on gaussian integration over a multifaceted crystal model was applied. Data collection and refinement parameters are given in Tables S1 and S2. The structure was solved by direct methods using SHELXT,[45] which revealed the positions of all not disordered non-hydrogen atoms of the title compound. The non-hydrogen atoms were refined anisotropically. All H-atoms were placed in geometrically calculated positions and refined using a riding model where each H-atom was assigned a fixed isotropic displacement parameter with a value equal to 1.2Ueq of its parent atom (1.5Ueq for the methyl groups and water). Refinement of the structure was carried out on F^2 using full-matrix least-squares procedures, which minimized the function $\sum w(F_o^2 - F_c^2)^2$. The weighting scheme was based on counting statistics and included a factor to downweight the intense reflections. All calculations were performed using the SHELXL-2014/7[46] program. Further crystallographic details are compiled in Tables S1 and S2. Crystallographic data for all structures have been deposited with the Cambridge Crystallographic Data Centre (CCDC) as supplementary publication numbers **6b** (1993400) and **7b** (1993401).

Acknowledgements

We thank the Swiss National Science Foundation for financial support of this work and the X-ray service of the University of Bern for crystallographic analyses (200020_182663 and R'equip 206021_128724 and 206021_170755).

Supporting Material Available: NMR spectra of all new compounds; crystallographic details.

References

1. U. Lüning, *Angew. Chem. Int. Ed.* **51**, 8163 (2012).
2. M. Vlatković, B. S. L. Collins, and B. L. Feringa, *Chem. Eur. J.* **22**, 17080 (2016).
3. V. Blanco, D. A. Leigh, and V. Marcos, *Chem. Soc. Rev.* **44**, 5341 (2015).
4. T. Imahori and S. Kurihara, *Chem. Lett.* **43**, 1524 (2014).
5. B. M. Neilson and C. W. Bielawski, *ACS Catal.* **3**, 1874 (2013).
6. G. Romanazzi, L. Degennaro, P. Mastroiilli, and R. Luisi, *ACS Catal.* **7**, 4100 (2017).
7. T. Traut, *Allosteric Regulatory Enzymes* (New York, 2008).
8. S. L. Balof, S. J. P. Pool, N. J. Berger, E. J. Valente, M. Shiller, and H.-J. Schanz, *Dalton Trans.* 5791 (2008).
9. P. Thordarson, E. J. A. Bijsterveld, A. E. Rowan, and R. J. M. Nolte, *Nature* **424**, 915 (2003).
10. Y. Sohtome, S. Tanaka, K. Takada, T. Yamaguchi, and K. Nagasawa, *Angew. Chem. Int. Ed.* **49**, 9254 (2010).
11. X. Tian, C. Cassani, Y. Liu, A. Moran, A. Urakawa, P. Galzerano, E. Arceo, and P. Melchiorre, *J. Am. Chem. Soc.* **133**, 17934 (2011).
12. B. M. Neilson and C. W. Bielawski, *ACS Catal.* **3**, 1874 (2013).
13. R. S. Stoll and S. Hecht, *Angew. Chem. Int. Ed.* **49**, 5054 (2010).
14. J. Barber, *Chem. Soc. Rev.* **38**, 185 (2009).
15. R. Göstl, A. Senf, and S. Hecht, *Chem. Soc. Rev.* **43**, 1982 (2014).
16. N. K. Rana, S. Selvakumar, and V. K. Singh, *J. Org. Chem.* **75**, 2089 (2010).
17. J. Wang and B. L. Feringa, *Science* **331**, 1429 (2011).
18. S. Erbas-Cakmak, D. A. Leigh, C. T. McTernan, and A. L. Nussbaumer, *Chem. Rev.* **115**, 10081 (2015).
19. P. G. Jessop, D. J. Heldebrant, X. Li, C. A. Eckert, and C. L. Liotta, *Nature* **436**, 1102 (2005).
20. O. Coulembier, S. Moins, R. Todd, and P. Dubois, *Macromolecules* **47**, 486 (2014).
21. S. L. Balof, S. J. P. Pool, N. J. Berger, E. J. Valente, A. M. Shiller, and H. J. Schanz, *Dalton Trans.* 5791 (2008).
22. S. L. Balof, B. Yu, A. B. Lowe, Y. Ling, Y. Zhang, and H. J. Schanz, *Eur. J. Inorg. Chem.* 1717 (2009).
23. L. H. Peeck, S. Leuthäusser, and H. Plenio, *Organometallics* **29**, 4339 (2010).
24. Y. Ryu, G. Ahumada, and C. W. Bielawski, *Chem. Commun.* **55**, 4451 (2019).
25. A. J. Teator and C. W. Bielawski, *J. Polym. Sci. Part A Polym. Chem.* **55**, 2949 (2017).
26. A. J. Teator, H. Shao, G. Lu, P. Liu, and C. W. Bielawski, *Organometallics* **36**, 490 (2017).
27. D. N. Lastovickova, A. J. Teator, H. Shao, P. Liu, and C. W. Bielawski, *Inorg. Chem. Front.* **4**, 1525 (2017).

28. J. D. Crowley, A. Lee, and K. Kilpin, *Aust. J. Chem.* **64**, 1118 (2011).
29. Á. Vivancos, C. Segarra, and M. Albrecht, *Chem. Rev.* **118**, 9493 (2018).
30. A. Petronilho, A. Vivancos, and M. Albrecht, *Catal. Sci. Technol.* **7**, 5766 (2017).
31. A. Petronilho, J. A. Woods, H. Mueller-Bunz, S. Bernhard, and M. Albrecht, *Chem. Eur. J.* **20**, 15775 (2014).
32. M. Meldal and C. W. Tomoe, *Chem. Rev.* **108**, 2952 (2008).
33. M. Olivares, C. J. M. van der Ham, V. Mdluli, M. Schmidtendorf, H. Müller-Bunz, T. W. G. M. Verhoeven, M. Li, J. W. (Hans) Niemantsverdriet, D. G. H. Hetterscheid, S. Bernhard, and M. Albrecht, *Eur. J. Inorg. Chem.* 801, (2020).
34. M. Delgado-Rebollo, D. Canseco-Gonzalez, M. Hollering, H. Mueller-Bunz, and M. Albrecht, *Dalton Trans.* **43**, 4462 (2014).
35. M. Valencia, H. Müller-Bunz, R. A. Gossage, and M. Albrecht, *Chem. Commun.* **52**, 3344 (2016).
36. Z. Mazloomi, R. Pretorius, O. Pàmies, M. Albrecht, and M. Diéguez, *Inorg. Chem.* **56**, 11282 (2017).
37. Á. Vivancos, A. Petronilho, J. Cardoso, H. Müller-Bunz, and M. Albrecht, *Dalton Trans.* **47**, 74 (2018).
38. B. Bagh and D. W. Stephan, *Dalton Trans.* **43**, 15638 (2014).
39. S. Sabater, H. Müller-Bunz, and M. Albrecht, *Organometallics* **35**, 2256 (2016).
40. J.-W. Liu, X.-H. Li, Z.-X. Wang, H.-J. Guo, and Q.-Y. Hu, *Chem. Res. Chinese Univ.* **25**, 791 (2009).
41. K. Vollhart, C. Peter, and N. Schore, *Organic Chemistry, Structure and Function*, 5th Ed. (W. H. Freeman and Company, 2007).
42. J. McMurry, *Fundamentals of Organic Chemistry*, 3rd Ed. Co (Pacific Grove, CA: Brooks/Cole Publishing Company, 1994).
43. CrysAlisPro (Version 1.171.34.44) Oxford Diffraction Ltd., Yarnton, Oxfordshire, UK, 2010.
44. P. Macchi, H. B. Bürgi, A. S. Chimpri, J. Hauser, and Z. Gál, *J. Appl. Cryst.* **44**, 763 (2011).
45. G. M. Sheldrick, *Acta Crystallogr. A* **71**, 3 (2015).
46. G. M. Sheldrick, *Acta Crystallogr. C* **71**, 3 (2015).